



Effects of Dy substitution for Ce on transport properties of $(\text{Pb}_2\text{Cu})\text{Sr}_2\text{Dy}_x\text{Ce}_{n-x-\delta}\text{Cu}_2\text{O}_{2n+6}$ ($n = 5, 6$) epitaxial films

Sumio Ikegawa^{a,*}, Kohei Nakayama^a, Masao Arai^b

^a Corporate Research and Development Center, Toshiba Corporation, 1 Komukai Toshiba-cho, Saiwai-ku, Kawasaki 212-8582, Japan

^b National Institute for Materials Science, Tsukuba, Ibaraki 305-0044, Japan

Received 31 May 2002; received in revised form 29 July 2002; accepted 5 August 2002

Abstract

The crystal structure, in-plane resistivity, and thermopower for $(\text{Pb}_2\text{Cu})\text{Sr}_2\text{Dy}_x\text{Ce}_{n-x-\delta}\text{Cu}_2\text{O}_{2n+6}$ (Pb-32n2 phase, $n = 5$ or 6) have been studied as a function of Dy content, x , in the fluorite block to ascertain the limit of hole doping. The samples were grown by sequential deposition using the molecular beam epitaxy technique. For $n = 5$, a single phase sample was obtained in the range of $0.9 < x < 3.2$. The hole density was estimated from the thermopower. With increasing x from 1.0 to 1.6, the hole density slightly increased. For the sample with $x > 1.6$, resistivity and thermopower abruptly increased beyond the value for $x = 1.0$, suggesting the electronic state change without changes in crystallinity. The ab-initio electronic structure calculations suggest that the substitution of Ln^{3+} for Ce^{4+} in the fluorite block has two effects detrimental to conducting properties and superconductivity: (a) creation of vacancy or the hole trap at the oxygen site in the fluorite block, and (b) decrease of the distance between Cu and apical oxygen. These effects may explain the experimental results. They are also considered to be the reasons for the absence of superconductivity in the layered cuprates having a multiple fluorite-type block with $n \geq 3$.

© 2002 Elsevier Science B.V. All rights reserved.

PACS: 74.72.Jt; 74.80.Dm; 74.10.+v

Keywords: Hole doping; Fluorite block; MBE; Electronic structure calculation; Thermopower

1. Introduction

A variety of layered cuprates having a fluorite-type block between a pair of CuO_2 planes has been synthesized [1], since the discovery of $(\text{Nd,Ce,Sr})_2\text{CuO}_4$ (T^* phase) superconductor [2]. These compounds are expressed by the general formula, $\text{M-}m2n2$, where M is the representative element in the charge reservoir layer which sits between apical

oxygens of CuO_5 type pyramid layer and m is the number of atomic layers of the charge reservoir layer. The number, n , is the number of atomic layers of rare earth element in the fluorite block between a pair of CuO_2 planes. The number n can be an arbitrary integer larger than two, which corresponds to multiple-stacked fluorite-type block.

Among the $\text{M-}m2n2$ compounds with $n = 2$, many superconductors have been discovered, such as $(\text{Nd,Ce,Sr})_2\text{CuO}_4$ (T^* phase or 0222 phase) [2], $(\text{RE,Ce})_2(\text{Ba,RE})_2\text{Cu}_3\text{O}_{10}$ ($\text{RE} = \text{Nd, Sm, Eu, Cu-1222 phase}$) [3], and $\text{Bi}_2\text{Sr}_2(\text{RE,Ce})_2\text{Cu}_2\text{O}_{10}$

* Corresponding author. Fax: +81-44-520-1275.

E-mail address: sumio.ikegawa@toshiba.co.jp (S. Ikegawa).

(Bi-2222 phase) [4]. The highest T_c ever reported for $n = 2$ compounds is 75 K, which was obtained for $(\text{Hg}_{0.75}\text{W}_{0.25})\text{Sr}_2(\text{Gd}_{1.5}\text{Ce}_{0.5})\text{Cu}_2\text{O}_z$ [(Hg,W)-1222 phase] [5]. This T_c is lower than the maximum T_c for $(\text{Hg}_{0.8}\text{W}_{0.2})\text{Sr}_2(\text{Ca}_{0.6}\text{Y}_{0.4})\text{Cu}_2\text{O}_z$ ($T_c = 94$ K) [6]. It seems that the fluorite-type block is less favorable for superconductivity than the (Ca,Y) layer [5]. Moreover, it is difficult for the M- $m2n2$ compounds with $n \geq 3$ to exhibit superconductivity [7–10] with one exception [11]. The reason for this requires clarification.

Generally, hole doping in the layered cuprate having a fluorite-type block is difficult. Hole carriers are doped in these compounds by the following two methods mainly: (i) oxygen doping to the charge reservoir layer sometimes under high oxygen pressure, (ii) substitution of Ln^{3+} for Ce^{4+} in the fluorite-type block, where Ln is a rare earth element with trivalence. Oxygen-content dependence was reported for Cu-1222 phase [12], and Ln^{3+} -composition dependence was reported for 0222 phase [13]. There are few works in which hole doping for the M- $m2n2$ compounds with $n \geq 3$ is studied systematically.

The M- $m2n2$ family is not merely one variation of layered cuprates. This family potentially has a new function which enables arbitrary and precise control of Josephson coupling between the CuO_2 planes, since the distance between a pair of CuO_2 planes across the fluorite block can be chosen arbitrarily [14]. For that purpose, we have grown $(\text{Pb}_2\text{Cu})\text{Sr}_2(\text{Ln,Ce})_n\text{Cu}_2\text{O}_{6+2n-d}$ ($n = 3-8$, Ln = rare earth element with trivalence, $d =$ oxygen nonstoichiometry, Pb- $32n2$ phase) single-phase epitaxial films [14]. The dependence on growth condition was investigated [15]. And, we reported the in-plane transport properties of Pb- $32n2$ films with $n = 3$ and 5 [16,17]. It should be noted that the Pb-3222 phase was reported to be a superconductor with $T_c \sim 20$ K [18,19], and the Pb- $32n2$ phase with $n \geq 3$ has not exhibited superconductivity to date [9,17]. Recently, we have successfully grown $[(\text{Pb-}32n2)_1(\text{Pb-}3212)_3]_9$ ($n = 3, 4, 6$) superconducting superlattices in which the distances between the superconducting layers are controlled at the shortest interval so far achieved [20,21]. If the superconducting order parameter extends to the CuO_2 plane in the Pb- $32n2$ phase with $n \geq 3$,

the CuO_2 plane and the fluorite block seem to form an ideal superconductor–insulator interface. To achieve this, the CuO_2 planes in the Pb- $32n2$ phase should be doped with carriers of the same level as the superconductor [17]. So, in order to realize the new function, systematic study of hole doping for the Pb- $32n2$ phase with $n \geq 3$ is needed.

The Pb- $32n2$ family has the [PbO–Cu–PbO] charge reservoir layer. Excess oxygen in [PbO–Cu–PbO] block layer is harmful for superconductivity in Pb-3212 phase, since charge is redistributed and the majority of holes are absorbed into [PbO–Cu–PbO] block layer [22]. Actually, superconductivity in the Pb-3212 and Pb-3222 phases was obtained after the heat treatment under a rather reducing atmosphere. Therefore, the only way of hole doping to the Pb- $32n2$ phase with $n \geq 2$ is substitution of Ln^{3+} for Ce^{4+} in the fluorite-type block. In this paper, we report on the effect of substitution of Dy^{3+} for Ce^{4+} in the Pb-3252 and Pb-3262 phases.

2. Experimental

The c -axis oriented films with nominal compositions of $(\text{Pb}_2\text{Cu})\text{Sr}_2\text{Dy}_x\text{Ce}_{5-x-\delta}\text{Cu}_2\text{O}_{16-d}$: $x = 0-3.88$ (Pb-3252 phase), and $(\text{Pb}_2\text{Cu})\text{Sr}_2\text{Dy}_x\text{Ce}_{6-x-\delta}\text{Cu}_2\text{O}_{18-d}$: $x = 1.09-1.87$ (Pb-3262 phase) were grown by the molecular beam epitaxy (MBE) technique. Pb, Sr, Ca, Dy, Ce, and Cu metals were evaporated from the effusion cells onto a SrTiO_3 (001) surface. The growth temperature was 953 K. The flux density from each metal source was adjusted individually prior to growth. The fluxes of each metal were supplied sequentially to the substrate in accordance with the stacking order of elements in the Pb- $32n2$ crystal structure. The shuttering sequence was repeated 25 times, corresponding to the film thickness of 67–74 nm. For the growth of the Pb-3252 and Pb-3262 films, an undercoat consisting of three-unit-cell-thick Pb-3212 phase was deposited on the substrate surface. The composition of the undercoat was chosen to give low carrier concentration and high resistivity. Resistivity and thermopower for the undercoat alone were measured. The contribution of the undercoat was estimated to be less than 0.1% of

the resistivity and less than 1% of the thermopower. Pure ozone gas [23] was continuously supplied to the substrate during growth: the flux density of O₃ molecules was estimated to be $6 \times 10^{18} \text{ s}^{-1} \text{ m}^{-2}$ on the substrate. The oxygenation conditions during growth and during the cooling process after growth were optimized to obtain low resistivity [15,17]. As a result, the valence state of Pb ion in the films is supposed to be +2 [22].

After the film growth, the phases present were determined by X-ray diffraction (XRD), using Cu K α radiation. Then the sample was cut into two or three pieces: the first piece for chemical analysis, the second piece for resistivity measurement, and the third piece, if any, for thermopower measurement. The chemical composition of the films was analyzed by inductively coupled plasma (ICP) emission spectroscopy and was expressed as the number of atoms per *ab*-plane unit cell area (0.148 nm²) per shuttering cycle. The ideal compositions for Pb-3252 phase are expressed as Pb₂Sr₂Dy_{*x*}Ce_{5-*x*}Cu₃O₁₆. The total accuracy of the ICP measurements was estimated to be within 2%. The compositions of films for Pb-3252 experiments are given in Table 1. The Sr compositions were not directly measured, but estimated from the flux monitor, since the dissolve procedure for these films also dissolves the SrTiO₃ substrate.

In Table 1, there are discrepancies between the film compositions and the ideal compositions suggesting the existence of many kinds of defects in the films as follows. First, it is hard for Pb to be

fully incorporated into the film up to the ideal value, since the vapor pressure of PbO and Pb are higher than 0.1 Pa at the growth temperature. A marked Pb deficiency was observed in the samples A, B, C, and N, in which the desired crystal structure according to the shuttering sequence was not grown. In the other samples, Pb was 0–25% deficient in terms of the stoichiometric compositions. The Sr-rich and Cu-deficient conditions were chosen to prevent the precipitation of Cu₂O [24,25]. It is possible for surplus Sr to occupy the Pb site vacancies since the ionic radius of Sr²⁺ is nearly equal to that of Pb²⁺. These defects with a similar level were also included in the (Pb₂Cu)Sr₂Dy_{1-*y*}Ca_{*y*}Cu₃O₈ (Pb-3212 phase) film samples. These may be harmful to superconductivity but the effects are so weak that the Pb-3212 films show superconductivity [24]. In spite of the existence of these defects, the hole-doping characteristics by the cation substitution in (Pb₂Cu)Sr₂Dy_{1-*y*}Ca_{*y*}Cu₃O₈ film samples appeared to be normal: the hole density was small ($p = 0.06$) for $y = 0$ and increased to $p = 0.12$ for $y = 0.21$ [17].

The ideal composition of the rare earth element, *w*, in a unit cell of (Pb₂Cu)Sr₂(Dy,Ce)_{*w*}Cu₃O_{*z*} should be 5.0 for the Pb-3252 phase. The Pb-3252 films, however, were grown for $w = 3.8$ – 4.7 [17]. This suggests that cation deficiency, δ , within the range between 0.3 and 1.2 exists in the fluorite block of Pb-32*n*2 phase films with $n = 3$ – 8 [17]. Then in the Pb-3252 samples, w was adjusted to the value of 3.8–4.7.¹ Actually, the target composition was chosen to be $w = 4.2$, and the resultant deviations were within $\pm 8\%$ except for the sample A.¹ It is considered to be hard for Sr²⁺ and Pb²⁺ to occupy the cation vacancies in the fluorite block, since these ions are too large: the ionic radii with the coordination number of eight for Ce⁴⁺, Dy³⁺, Sr²⁺, and Pb²⁺ are 0.097, 0.1027, 0.126, and 0.129 nm, respectively [26]. On the other hand, it is supposed to be hard for Cu ion to

Table 1
Dy content (*x*) and compositions of the film samples

Sample	<i>x</i>	Compositions
A	0	Pb _{0.81} Sr _{2.1} Ce _{3.57} Cu _{2.86} O _{<i>y</i>}
B	0.08	Pb _{1.09} Sr _{2.2} Dy _{0.08} Ce _{4.33} Cu _{2.78} O _{<i>y</i>}
C	0.97	Pb _{1.36} Sr _{2.2} Dy _{0.97} Ce _{3.31} Cu _{2.81} O _{<i>y</i>}
D	0.97	Pb _{1.65} Sr _{2.2} Dy _{0.97} Ce _{2.95} Cu _{2.91} O _{<i>y</i>}
E	1.06	Pb _{1.60} Sr _{2.2} Dy _{1.06} Ce _{3.19} Cu _{3.08} O _{<i>y</i>}
F	1.33	Pb _{1.53} Sr _{2.2} Dy _{1.33} Ce _{3.03} Cu _{2.91} O _{<i>y</i>}
G	1.46	Pb _{1.63} Sr _{2.2} Dy _{1.46} Ce _{2.59} Cu _{3.02} O _{<i>y</i>}
H	1.47	Pb _{1.69} Sr _{2.1} Dy _{1.47} Ce _{2.52} Cu _{2.97} O _{<i>y</i>}
I	1.64	Pb _{1.57} Sr _{2.2} Dy _{1.64} Ce _{2.42} Cu _{2.91} O _{<i>y</i>}
J	1.79	Pb _{1.76} Sr _{2.2} Dy _{1.79} Ce _{2.28} Cu _{2.91} O _{<i>y</i>}
K	2.02	Pb _{1.93} Sr _{2.2} Dy _{2.02} Ce _{2.45} Cu _{3.02} O _{<i>y</i>}
L	3.09	Pb _{2.09} Sr _{2.2} Dy _{3.09} Ce _{1.30} Cu _{3.01} O _{<i>y</i>}
M	3.32	Pb _{1.65} Sr _{2.2} Dy _{3.32} Ce _{0.74} Cu _{2.73} O _{<i>y</i>}
N	3.88	Pb _{1.31} Sr _{2.2} Dy _{3.88} Cu _{2.84} O _{<i>y</i>}

¹ It should be noted that the value of w for sample A was out of this range because of the poor control of Ce flux. If the crystal grew according to the shuttering sequence, the Pb-3242 phase would be grown in the sample A.

occupy the cation vacancies in the fluorite block, since Cu ion is too small.

For transport measurements, silver was evaporated onto the film for contacts. In-plane resistivity measurements were carried out by a conventional dc four-probe method in the temperature range between 1.5 and 420 K. In-plane thermoelectric power was measured by a steady-state technique at temperatures between 200 and 320 K. The temperature and temperature gradient across the sample were measured using a calibrated Cernox sensor (Lake Shore Cryotronics Inc.) and two pairs of Cu–Constantan thermocouples, respectively. Cu wires of 50- μm diameter were used as the reference metal.

The hole density, p , per $[\text{CuO}]^{p+}$ is an important parameter, determining both the normal-state and superconducting-state properties of layered cuprates. Tallon et al. [27] found a universal relation between the thermopower at 290 K, S_{290} and p , for various layered cuprates. Thus, S_{290} is thought to be a measure of p in all the layered cuprates, though an exception was recently found [28]. We used the following equations derived from Tallon's universal curve to evaluate the hole concentration of the film samples [17]:

$$p = -\frac{1}{32.4} \ln \left(\frac{S_{290} [\mu\text{V/K}]}{372 [\mu\text{V/K}]} \right) \quad \text{for } 0 < p \leq 0.04,$$

$$p = -\frac{1}{25.3} \ln \left(\frac{S_{290} [\mu\text{V/K}]}{278 [\mu\text{V/K}]} \right) \\ \text{for } 0.04 < p \leq 0.10,$$

$$p = -\frac{1}{38.1} \ln \left(\frac{S_{290} [\mu\text{V/K}]}{992 [\mu\text{V/K}]} \right) \\ \text{for } 0.10 < p \leq 0.155.$$

3. Results

3.1. Structural chemistry of Pb-3252 films

First, we investigate the composition range of rare earth element for obtaining a Pb-3252 single phase. Fig. 1 shows XRD patterns for the films with nominal compositions of $(\text{Pb}_2\text{Cu})\text{Sr}_2\text{Dy}_x$ -

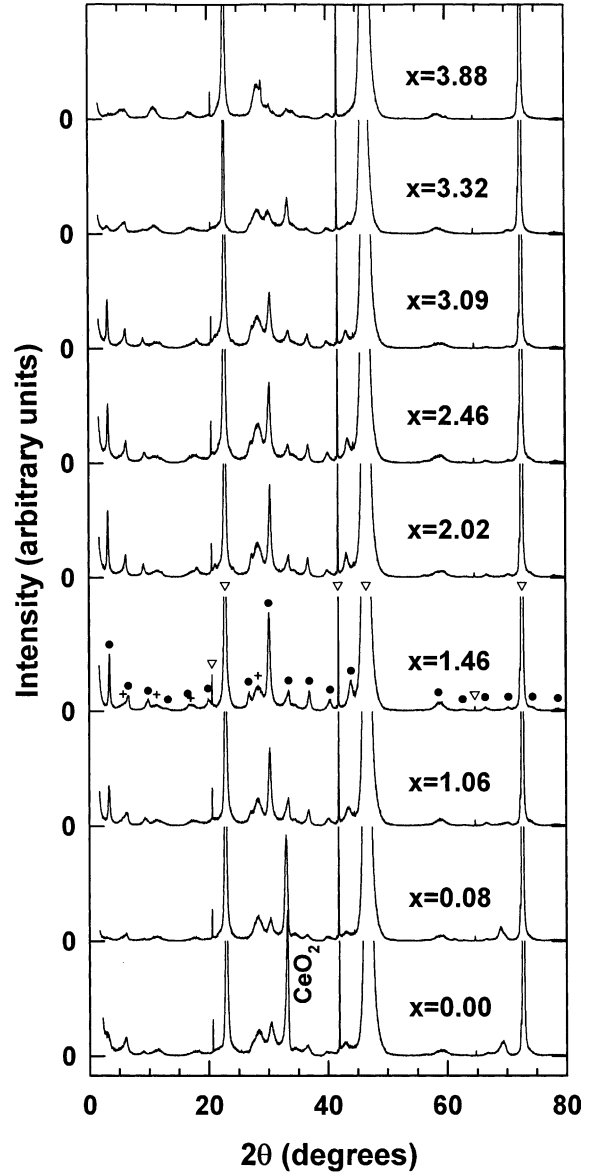


Fig. 1. XRD patterns for films with various Dy content, x . Closed circles indicate the peak positions for the Pb-3252 phase. Open triangles indicate the peaks due to the substrate and crosses indicate the peaks due to the undercoat.

$\text{Ce}_{5-x-\delta}\text{Cu}_2\text{O}_{16-d}$ with various Dy content, x . In the XRD pattern for $x = 1.46$, the peak positions for the Pb-3252 phase are indicated by closed circles. In this figure, open triangles and crosses indicate the peaks due to the substrate and the

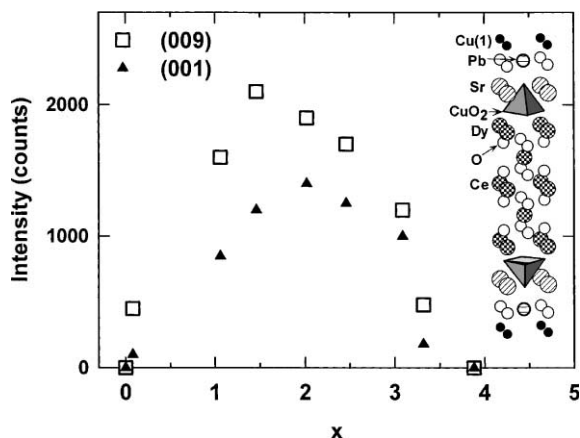


Fig. 2. XRD intensity vs. Dy content, x , for film samples. Open squares indicate the intensity of (009) peak and closed triangles indicate the intensity of (001) peak of the Pb-3252 phase. Inset shows the crystal structure of Pb-3252 phase.

undercoat (Pb-3212 phase), respectively. The XRD pattern for $x = 1.46$ qualitatively agreed with that of the calculated ones assuming the ideal crystal structure of Pb-3252 phase, as reported in the previous paper [17]. There are no peaks due to impurity phases.

On the other hand, the films with $x \geq 3.32$ and $x \leq 0.08$ were mixed phases chiefly composed of $\text{Dy}_x\text{Ce}_{1-x}\text{O}_{2-d}$ and the Pb-3212 phase.² From Fig. 1, the XRD intensities of (001) and (009) reflections of Pb-3252 structure are plotted as a function of x in Fig. 2. The (001) peak is positioned at $2\theta = 3.3^\circ$. The (009) peak is the main peak positioned at $2\theta = 30^\circ$. Fig. 2 shows that the composition range where the Pb-3252 phase is stably synthesized is $0.9 < x < 3.2$.

3.2. Transport properties of Pb-3252 films

Temperature dependence of resistivity for the single-phase samples of Pb-3252 phase is shown in Fig. 3. All the samples show insulating behavior.

² Judging from the rare earth composition, not the Pb-3252 phase but the Pb-3242 phase would be grown in the sample A, if the crystal grew according to the shuttering sequence (see footnote 1). The sample A showed that the single Pb-32n2 phase did not grow for $x = 0$.

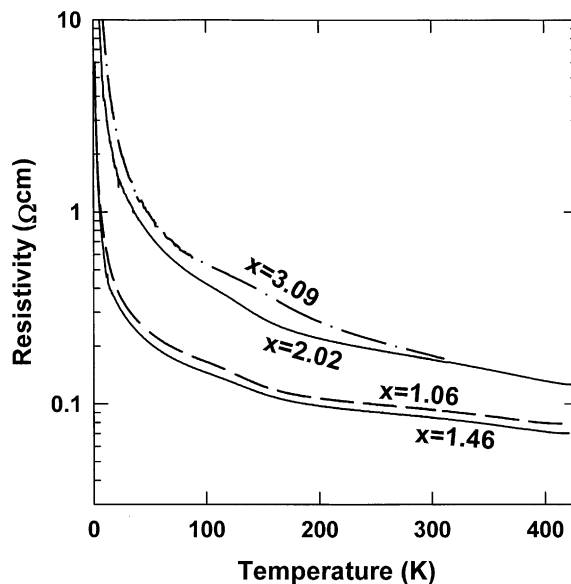


Fig. 3. Temperature dependence of resistivity for Pb-3252 films with various Dy content, x .

To understand the nature of insulating behavior, the resistivity data were compared with the thermal activation-type model $\rho \propto \exp(E/k_B T)$ and the variable range hopping (VRH) models $\rho \propto \exp[(T_0/T)^{1/(d+1)}]$. The VRH model with $d = 2$ was the fittest model for the data. Fig. 4 shows the logarithm of resistivity of the sample with $x = 1.06$ as a function of $T^{-1/3}$. As is evidenced by the straight line in Fig. 4, $\rho \propto \exp(T_0/T)^{1/3}$ below 50 K. Transport properties of Pb-3252 phase are characterized by the law, $\rho \propto \exp(T_0/T)^{1/3}$, within a wider temperature range than other transition metal oxides, such as Ca_2RuO_4 and SmNiO_3 . This may be attributed to two-dimensional VRH transport. In this mechanism, $T_0 = 3^3 / [\pi k_B N(E_F) \xi^2]$, where $N(E_F)$ is the density of states at Fermi level and ξ is the localization length [29]. The value of T_0 was 150 K for the sample in Fig. 4, which is smaller than the reported value for $\text{PrBa}_2\text{Cu}_3\text{O}_7$ [30,31]. This suggests that the localization of carriers in the Pb-3252 film is weaker than that of $\text{PrBa}_2\text{Cu}_3\text{O}_7$.

The sample with $x = 1.46$ has the lowest resistivity among the samples in Fig. 3. Next, we see the dependence on Dy composition, x , of resistivity, which is summarized in Fig. 5. We focus on

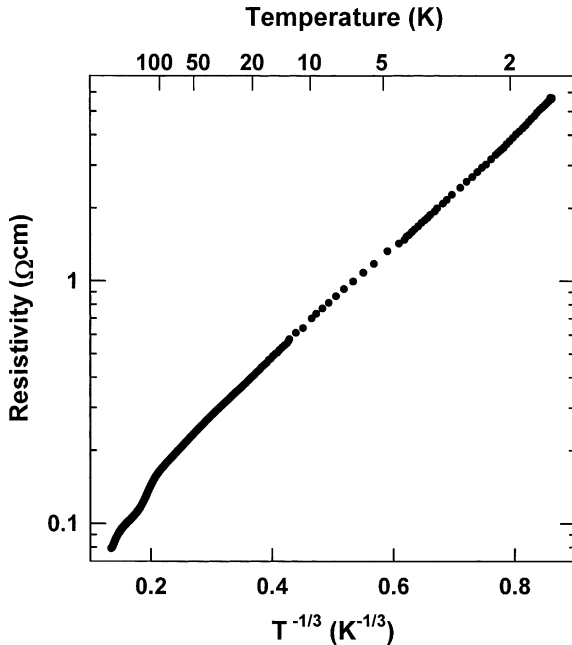


Fig. 4. Resistivity vs. $T^{-1/3}$ for Pb-3252 film with $x = 1.06$.

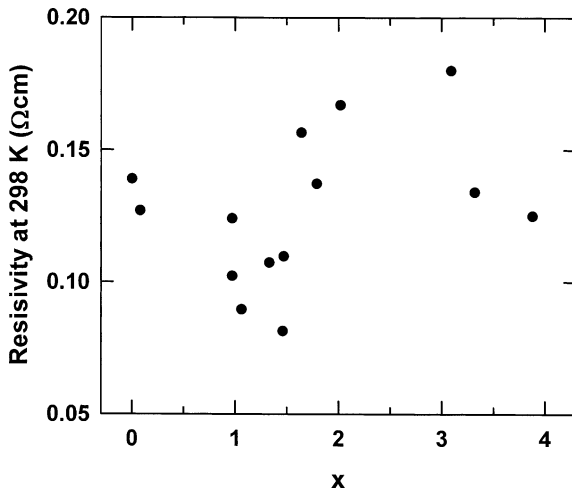


Fig. 5. Resistivity at 298 K for film samples as a function of Dy content, x .

the composition range of $0.9 < x < 3.2$ where the single phase of Pb-3252 was synthesized. From the simple calculation of the valence assuming $z = 0$ and $\delta = 0$ in $(\text{Pb}_2\text{Cu})\text{Sr}_2\text{Dy}_x\text{Ce}_{5-x-\delta}\text{Cu}_2\text{O}_{16-d}$ (Pb-3252 phase), $x = 1$ corresponds to the parent compound and the hole density p would increase with x following the relation $p = (x - 1)/2$. Then,

we can expect that resistivity at room temperature decreases with increasing x from 1.0. When x increases from 1.0 to 1.5 in Fig. 5, resistivity shows a tendency to decrease, though the data points are scattered. However, when x increases above 1.6, resistivity is larger than that around $x = 1.0$. This implies that mobile holes are not introduced effectively by the Dy substitution above $x = 1.6$.

Thermopower for the selected samples (samples D, F, H, I, and J in Table 1) was measured to estimate the hole density. Fig. 6 shows the thermopower at 290 K and the estimated hole density. ³ The hole density increases with increasing x from 0.97 to 1.47, as expected. However, this trend fails to continue for $x > 1.6$. Mobile holes are not introduced effectively by the Dy substitution above $x = 1.6$.

Within the range of $0.9 < x < 1.6$, the substitution of Dy^{3+} for Ce^{4+} increased the hole density, but the densities obtained disagreed with the expectation from the simple calculation of the valence, regarding the following two points [17]. First, a self-doping of holes was observed in the sample with $x \sim 1$ where we intended to make the parent compound before hole doping. Second, the hole densities for the samples with $x = 1.33$ and 1.47 were smaller than expected. This means that the efficiency of hole doping with cation substitution is very low.

Combining Figs. 2, 5, and 6, it appears that the decrease of resistivity and thermopower with increasing x from around 1.0 to 1.5 can be caused by the increase of crystallinity. Next, we compare the XRD intensities for $x < 1.6$ and those for $x > 1.6$ in Fig. 2. The (001) intensities for $x = 2.02$ and 2.46 are larger than those for $x = 1.06$ and 1.46. The (009) intensities for $x = 2.02$ and 2.46 are

³ Thermopower data for the Pb-3252 phase samples in this paper are somewhat larger than the previously reported values in Ref. [17]. The discrepancy between the present and previous paper is mainly due to the difference in the growth temperature. The growth temperature in this paper was optimized to obtaining reproducible superconductivity in the superlattices and is twenty degrees lower than that in Ref. [17]. The growth temperature in this paper is considered to be the temperature where the interdiffusion of atoms between adjacent unit cells is not significant.

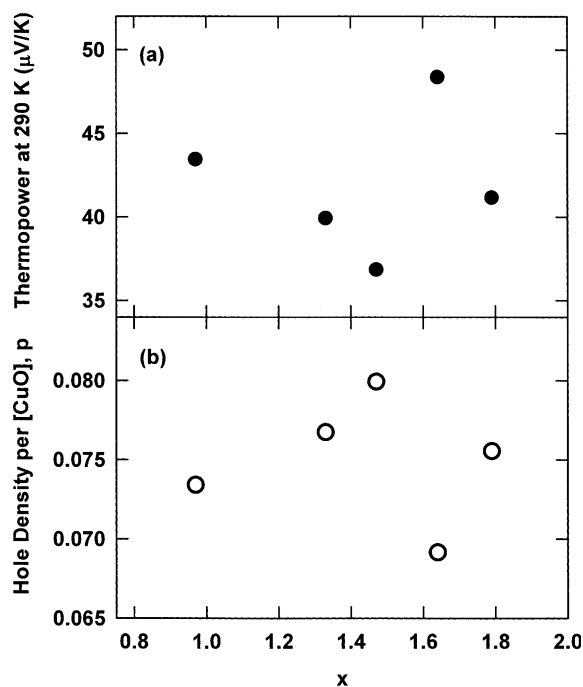


Fig. 6. Dependence on Dy content, x , of (a) thermopower at 290 K, and (b) estimated hole density, p , for Pb-3252 films.

larger than that for $x = 1.06$. So, the increase of resistivity and thermopower for $x > 1.6$ is not straightforwardly explained by the degradation of crystal. Thus, there may be changes in electronic state without the change in crystallinity when x exceeds 1.6.

3.3. Structural chemistry and transport properties of Pb-3262 films

Next, we examine the Pb-3262 phase, $(\text{Pb}_2\text{Cu})\text{-Sr}_2\text{Dy}_x\text{Ce}_{6-x-\delta}\text{Cu}_2\text{O}_{18-d}$, to check the universality of the above-mentioned results. Fig. 7 shows x -dependence of (a) XRD intensity, (b) thermopower and resistivity, and (c) the estimated hole density, p . Judging from XRD patterns, all the samples in Fig. 7 are the single phase of Pb-3262. The (001) peak is positioned at $2\theta = 3.0^\circ$ and the (0010) peak is the main peak positioned at $2\theta = 30^\circ$.

Resistivity and thermopower decrease with increasing x from 1.0 to 1.6 (Fig. 7(b)), consequently the estimated hole density increases with x up to

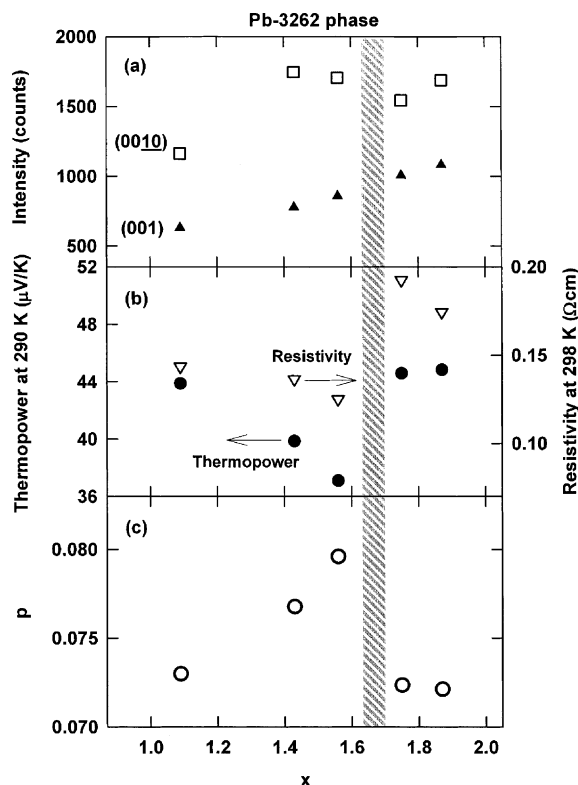


Fig. 7. The properties of Pb-3262 phase as a function of Dy content, x . (a) XRD intensity for (0010) and (001) peaks of Pb-3262 phase, (b) thermopower at 290 K and resistivity at 298 K, and (c) estimated hole density, p .

1.6 (Fig. 7(c)). These tendencies fail to continue for $x > 1.6$. Resistivity and thermopower for $x > 1.6$ are larger than those for $x = 1.09$. As shown in Fig. 7(a), the (001) XRD intensity for $x > 1.6$ is larger than that for $x < 1.6$ and the (0010) XRD intensity for $x > 1.6$ is larger than that for $x = 1.09$. Therefore, the increase of resistivity and thermopower for $x > 1.6$ is not attributed to the degradation of crystal. Therefore, the electronic state may change without changes in crystallinity, when x exceeds 1.6–1.7. The border is indicated by the hatched region in Fig. 7.

Similar to the case of Pb-3232 and Pb-3252 phases [17], a self-doping of holes was observed in the Pb-3262 sample with x around 1.0, where we intended to make the parent compound before hole doping, and the efficiency of hole doping with cation substitution was very low for $1.0 \leq x \leq 1.6$.

4. Discussion

The effects of Dy substitution for Ce in the Pb-3252 and Pb-3262 phases on the transport properties are summarized as follows. (1) Self-doping of holes was observed in the sample where we intended to make the parent compound before hole doping. (2) The hole density slightly increased with increasing x from 1.0 to 1.6 as expected, but a gain in the hole density by the cation substitution was smaller than expected. (3) For the sample with $x > 1.6$, resistivity and thermopower abruptly increased beyond the value for $x = 1.0$, suggesting the electronic state changed without changes in crystallinity. Thus, the limit of hole doping by the cation substitution in the Pb-32 n 2 phase was realized.

As mentioned in Section 2, the cation deficiency exists in the fluorite block. The cation deficiency may cause the self-doping [result (1)] [17]. The other discrepancies between the film compositions and the ideal compositions, such as Pb-deficiency, Sr-excess, and Cu-deficiency, and the possible occupation of the Pb sites by surplus Sr probably do not cause results (1) and (2), since the Pb-3212 phase with the similar defects showed the normal hole-doping characteristics as mentioned in Section 2.

Possible mechanisms for results (2) and (3) were revealed by the ab-initio electronic structure calculations. The electronic structure of the Pb-3232 phase was calculated within the local density approximation [32], using the WIEN97 package [33], which is based on the full-potential linear augmented plane wave method. The substitution of Ce^{4+} by Ln^{3+} lifts the energy level of the oxygen in the fluorite block. This is because electrostatic potential for electrons increases at the oxygen atoms in the fluorite block by substitution of the surrounding Ce^{4+} ions by Ln^{3+} . As a result, the oxygen atoms become unstable and the oxygen vacancies in the fluorite block may increase. This brings about the decrease of hole density. If the creation of oxygen vacancies is prevented by, for example, high-pressure oxygen treatment, the substitution with $x \gtrsim 2.0$ brings about the contribution of the oxygen $2p$ orbital in the fluorite block to the density of states at Fermi energy. It

means that a portion of doped holes are not released to the CuO_2 planes but are trapped in the fluorite block. Thus, the substitution of Ln^{3+} for Ce^{4+} in the fluorite block would not simply increase the hole density. This is consistent with the experimental results (2) and (3).

Another important suggestion from the calculation is a structure change. Structure optimization of Pb-3232 phase, $(\text{Pb}_2\text{Cu})\text{Sr}_2\text{Eu}_x\text{Ce}_{3-x}\text{Cu}_2\text{O}_{12}$: $x = 0$ and 2, was performed using the atomic force obtained by ab-initio electronic structure calculations. Detailed calculations are published elsewhere [34]. The initial structure chosen is the model structure described in the previous paper (Table III in Ref. [32]). The space group symmetry and lattice constants were fixed to the initial structure so that the atoms can move only in z -directions. Table 2 shows the distances between the selected layers in units of nm, which were obtained after the structure optimization. Also shown are the experimentally obtained distances in units of nm for Pb-3212 phase [35] as references. The most striking difference in the resultant structures between $x = 0$ and 2 is as follows. The distance between the $(\text{Ln}^{3+}, \text{Ce}^{4+})$ plane in the fluorite block and the adjacent CuO_2 plane becomes wider for $x = 2$ than that for $x = 0$. This behavior can be explained by the fact that the attractive static Coulomb potential between the $(\text{Ln}^{3+}, \text{Ce}^{4+})$ plane in the fluorite block and the adjacent CuO_2 plane becomes weak by the substitution of Ce^{4+} by Ln^{3+} . Consequently, the distance, z_2 between Cu in the CuO_2 plane and the apical oxygen becomes shorter for $x = 2$ than that for $x = 0$, whereas the buckling of CuO_2 plane, z_1 is nearly the same for $x = 0$ and 2. Here, z_1 was

Table 2
Calculated structure parameters in units of nm for the Pb-3232 phase

	Pb-3232 phase		Pb-3212 phase (experiment)
	$x = 0$	$x = 2$	
z_1	0.020	0.019	0.023
z_2	0.230	0.216	0.228

The z_1 is the buckling of CuO_2 plane defined as a difference of z coordinate of copper and oxygen in the CuO_2 plane. The z_2 is a distance between copper and apical oxygen. The experimentally obtained values for Pb-3212 phase [35] are also shown.

defined as a difference of z coordinate of copper and oxygen in the CuO_2 plane. As a result of this structural change, the bands which have weight on apical oxygen and $\text{Cu}3d_{3z^2-r^2}$ cross the Fermi energy for $x = 2$. This means that holes doped by the Ln^{3+} substitution with $x \sim 2$ are distributed not only to the states of $\text{O}2p_\sigma$ and $\text{Cu}3d_{x^2-y^2}$ orbitals within the CuO_2 plane but also to the states of apical oxygen and $\text{Cu}3d_{3z^2-r^2}$. This might be one of the reasons for the above-mentioned experimental result (3). Of course, further studies are needed to clarify whether the abrupt increase of resistivity and thermopower of the Pb-3252 and Pb-3262 phases at $x = 1.6$ is due to the rise of oxygen energy level, the structural change, or other mechanisms.

In the case of cuprate superconductors, it is thought that shrinkage of the bond length between Cu and apical oxygen brings about charge redistribution and T_c reduction [36]. This change is accompanied with the increase of normal state resistivity [36]. Ohta et al. found that the maximum T_c for a given crystal structure depends on the difference in the Madelung potentials ΔV_A for a hole between the apex and in-plane oxygen atoms [37]. The larger the ΔV_A , the more stable the holes induced into in-plane oxygen become and the larger the T_c becomes. Thus, the above-mentioned structural change of Pb-3232 phase with $x = 2.0$ is unfavorable for superconductivity. In other words, the large substitution of Ln^{3+} for Ce^{4+} in the fluorite block induces electronic states detrimental to superconductivity. This is considered to be one of the reasons for the absence of superconductivity in the layered cuprates having a multiple fluorite-type block with $n \geq 3$. However, the value of $p = 0.08$ obtained for the Pb-3252 and Pb-3262 films is sufficient for the occurrence of superconductivity in the case of $\text{La}_{2-x}\text{Sr}_x\text{CuO}_4$ [36]. A disordered potential in the CuO_2 plane is supposed to be one of the reasons for the absence of superconductivity, which was described in the previous paper [17]. The cation deficiency δ existing in the fluorite block may be one of the possible sources of the disordered potential [17].

The ab initio electronic structure calculations suggest that the substitution of Ln^{3+} for Ce^{4+} in the fluorite block, which would be expected to

increase mobile holes, has two effects detrimental to conducting properties and superconductivity: (a) creation of vacancy or the hole trap at the oxygen site in the fluorite block, because electrostatic potential for electrons increases at this site, (b) decrease of the distance between Cu and apical oxygen, since the attractive Coulomb potential between the (Ln^{3+} , Ce^{4+}) plane and the adjacent CuO_2 plane becomes weak. These suggestions can explain the experimental results in this paper. These effects are also crucial to superconductivity and transport properties in all the layered cuprates having a fluorite block.

In order to achieve precise control of the Josephson coupling along the c -axis using the $M\text{-}m2n2$ compounds, the CuO_2 planes adjacent to the multiple fluorite-type block should be doped with carriers to the same level as the superconductor [17]. It is realized that the substitution of Ln^{3+} for Ce^{4+} in the fluorite-type block reaches the limit for this purpose. So, the method of oxygen doping to the charge reservoir layer for hole doping should be adopted. The $[\text{PbO}\text{-Cu}\text{-PbO}]$ block layer is inappropriate for this method [22]. So, we have to search for compounds other than the Pb-32 $n2$ phase, which have the charge reservoir layer capable of doping holes by oxygen doping and multiple fluorite-type block layer.

5. Summary

We have studied the effect of Dy^{3+} substitution for Ce^{4+} on crystal structure, resistivity and thermopower for Pb-32 $n2$ phase films with $n = 5$ and 6. For $(\text{Pb}_2\text{Cu})\text{Sr}_2\text{Dy}_x\text{Ce}_{5-x-\delta}\text{Cu}_2\text{O}_{16-d}$, the single phase of Pb-3252 was stably synthesized for the Dy composition range of $0.9 < x < 3.2$. With increasing x from 1.0 to 1.6, the hole density slightly increased as expected, but a gain in the hole density was smaller than expected. For the sample with $x > 1.6$, resistivity and thermopower abruptly increased beyond the value for $x = 1.0$, suggesting the electronic state change without changes in crystallinity. The ab-initio electronic structure calculations suggest that the substitution of Ln^{3+} for Ce^{4+} in the fluorite block, which would be expected to increase mobile holes, has two effects

detrimental to conducting properties and superconductivity: (a) creation of vacancy or the hole trap at the oxygen site in the fluorite block, and (b) decrease of the distance between Cu and apical oxygen. These effects can explain the experimental results. They are also considered to be the reasons for the absence of superconductivity in the layered cuprates having a multiple fluorite-type block with $n \geq 3$. Thus, the limit of hole doping by the cation substitution in the Pb-32n2 phase was realized. In order to increase the hole density of the CuO_2 planes adjacent to the multiple fluorite-type block, a search for other compounds that have the charge reservoir layer capable of doping holes by oxygen doping is valid.

Acknowledgements

This study was supported by the Special Coordination Funds for Promoting Science and Technology from the Japanese Ministry of Education, Culture, Sports, Science and Technology, to which we are deeply indebted. We would like to thank Dr. M. Kawai of RIKEN, Dr. N. Terada of Kagoshima University and Dr. A. Fujimori of the University of Tokyo for illuminating discussion.

References

- [1] J. Hauck, K. Mika, *Physica C* 218 (1993) 316.
- [2] J. Akimitsu, S. Suzuki, M. Watanabe, H. Sawa, *Jpn. J. Appl. Phys.* 27 (1988) L1859.
- [3] H. Sawa, K. Obara, J. Akimitsu, Y. Matsui, S. Horiuchi, *J. Phys. Soc. Jpn.* 58 (1989) 2252.
- [4] Y. Tokura, T. Arima, H. Takagi, S. Uchida, T. Ishigaki, H. Asano, R. Beyers, A.I. Nazzal, P. Lacorre, J.B. Torrance, *Nature* 342 (1989) 890.
- [5] E. Kandyel, A. Yamamoto, S. Tajima, *Physica C* 341–348 (2000) 429.
- [6] K. Tang, Y. Qian, Z. Chen, Y. Zhang, *J. Supercond.* 9 (1996) 93.
- [7] T. Wada, A. Ichinose, H. Yamauchi, S. Tanaka, *Physica C* 171 (1990) 344;
T. Wada, K. Hamada, A. Ichinose, T. Kaneko, H. Yamauchi, S. Tanaka, *Physica C* 175 (1991) 529.
- [8] T. Wada, A. Ichinose, F. Izumi, A. Nara, H. Yamauchi, H. Asano, S. Tanaka, *Physica C* 179 (1991) 455.
- [9] A. Tokiwa, T. Oku, M. Nagoshi, Y. Shono, *Physica C* 181 (1991) 311.
- [10] T. Wada, A. Nara, A. Ichinose, H. Yamauchi, S. Tanaka, *Physica C* 192 (1992) 181.
- [11] C. Xianhui, D. Zhongfen, Q. Yitai, C. Zuyao, C. Zhaojia, C. Liezhao, *Phys. Rev. B* 48 (1993) 9799.
- [12] Y. Idemoto, Y. Hayakawa, N. Koura, J.W. Richardson Jr., C.-K. Loong, *Physica C* 329 (2000) 29.
- [13] M. Kosuge, K. Kurusu, *Jpn. J. Appl. Phys.* 28 (1989) L810.
- [14] S. Ikegawa, Y. Motoi, *Appl. Phys. Lett.* 68 (1996) 2430.
- [15] S. Ikegawa, Y. Motoi, *Physica C* 282–287 (1997) 673.
- [16] S. Ikegawa, Y. Motoi, *Physica C* 341–348 (2000) 1887.
- [17] S. Ikegawa, Y. Motoi, *Phys. Rev. B* 61 (2000) 6334.
- [18] A.L. Kharlanov, E.V. Antipov, L.M. Kovba, L.G. Akselrud, L.G. Muttik, A.A. Gippius, V.V. Moshchalkov, *Physica C* 169 (1990) 469.
- [19] H. Sasakura, K. Yoshida, K. Tagaya, S. Tsukui, T. Oka, R. Oshima, *J. Supercond.* 13 (2000) 401.
- [20] S. Ikegawa, Y. Motoi, M. Arai, *Trans. Mater. Res. Soc. Jpn.* 26 (2001) 1037.
- [21] S. Ikegawa, K. Nakayama, Y. Motoi, M. Arai, *Phys. Rev. B* 66 (2002) 014536.
- [22] N. Terada, S. Ikegawa, Y. Motoi, K. Obara, H. Ihara, *IEEE Trans. Appl. Supercond.* 11 (2001) 2707.
- [23] S. Hosokawa, S. Ichimura, *Rev. Sci. Instrum.* 62 (1991) 1614.
- [24] S. Ikegawa, Y. Motoi, T. Miura, *Physica C* 229 (1994) 280.
- [25] Y. Motoi, S. Ikegawa, *Appl. Phys. Lett.* 73 (1998) 987.
- [26] R.D. Shannon, *Acta Crystallogr. A* 32 (1976) 751.
- [27] S.D. Obertelli, J.R. Cooper, J.L. Tallon, *Phys. Rev. B* 46 (1992) 14928;
J.L. Tallon, C. Bernhard, H. Shaked, R.L. Hitterman, J.D. Jorgensen, *Phys. Rev. B* 51 (1995) 12911.
- [28] Y. Ando, Y. Hanaki, S. Ono, T. Murayama, K. Segawa, N. Miyamoto, S. Komiya, *Phys. Rev. B* 61 (2000) R14956.
- [29] N.F. Mott, E.A. Davis, in: *Electronic Processes in Non-crystalline Materials*, second ed., Clarendon, Oxford, 1979, p. 32.
- [30] B. Fisher, G. Koren, J. Genossar, L. Patlagan, E.L. Gartstein, *Physica C* 176 (1991) 75.
- [31] U. Kabasawa, Y. Tarutani, M. Okamoto, T. Fukazawa, A. Tsukamoto, M. Hiratani, K. Takagi, *Phys. Rev. Lett.* 70 (1993) 1700.
- [32] M. Arai, S. Ikegawa, *Trans. Mater. Res. Soc. Jpn.* 26 (2001) 1001.
- [33] P. Blaha, K. Schwarz, J. Luitz, WIEN97, A full potential linearized augmented plane wave package for calculating crystal properties, Karlheinz Schwartz, Techn. Universität Wien, Austria, 1999. ISBN 3-9501031-0-4.
- [34] M. Arai, S. Ikegawa, submitted for publication.
- [35] R.J. Cava, M. Marezio, J.J. Krajewski, W.F. Peck Jr., A. Santoro, F. Beech, *Physica C* 157 (1989) 272.
- [36] H. Sato, A. Tsukada, M. Naito, A. Matsuda, *Physica C* 341–348 (2000) 1767;
H. Sato, A. Tsukada, M. Naito, A. Matsuda, *Phys. Rev. B* 62 (2000) R799.
- [37] Y. Ohta, T. Tohyama, S. Maekawa, *Phys. Rev. B* 43 (1991) 2968.